Journal of Basrah Researches (Sciences) **52**(1), 254 (2026)
DOI: https://doi.org/10.56714/bjrs.52.1.18

Electrical and Optical Properties of Ppy and PANI Nanotubes Prepared by Core@ Shell Polymerization with Ag, ZnO, and Fe_3O_4 Nanoparticle

Fatima H. Malk[1,*], Hussein F. Hussein[2], Salah S. Al-luaibi[3]

[1]Polymer Research Center, Basrah University.
[2]Physics Department, College of Education for Pure Sciences, Basrah University.
[3]Chemistry department, College of Science, Basrah University.

ARTICLE INFO

Received 26 March 2026
Revised 01 May 2026
Accepted 07 May 2026
Published 30 June 2026

Keywords:

Core-Shell , Electrical Properties, Optical Properties, PPY, PANI, Electrical Conductivity

Citation: F. H. Malk et al., J. Basrah Res. (Sci.) **52**(1), 254 (2026).
DOI:https://doi.org/10.56714/bjrs.52.1.18

ABSTRACT

Polypyrrole (PPy), polyaniline (PANI) nanotubes, were prepared by core@ shell polymerisation with ZnO, Ag, and Fe_3O_4 nanoparticles to produce hybrid polymers i.e , PPy@(ZnO, Ag, Fe_3O_4) and PANI@(ZnO, Ag, Fe_3O_4). The hybrid polymers were characterized using infrared spectroscopy (IR) to confirm their chemical structures of polymers and using scanning & transmission electron microscopy (SEM and TEM) to confirm the morphology of the hybrid polymers and the nanotubes stricture.

The optical properties of the hybrid polymers were studied using a UV–visible spectrophotometer. The spectra showed broad absorption peaks in the range (383-386) nm and (430-433) nm for PANI@ZnO,Fe_3O_4,Ag and PPY@ZnO,Fe_3O_4,Ag respectively and the energy gaps of pure were found to be PPY and PANI 2.37eV and 2.5 eV respectively also showed that the energy gap decrease with incorporated nanoparticles.

The I-V characteristic of PANI and PPy and their core@ shell polymers with Zno,Fe_3O_4 and Ag nanoparticles were studied to determine how electricity travels in polymer membranes .The results showed a quasi-linear relationship between current and voltage, which indicates ohmic behavior, meaning that the electrical conductivity is stable and there are no large barriers that impede the transfer. The highest conductivity was observed for PANI @Zn ($789x10^{-4}$ S/m) and PPY @Ag ($273x10^{-4}$ S/m).

1.Introduction

Behaviour of polymeric materials has been the subject of numerous scholarly publications in recent years. It is particularly in its hybrid conductive polymers (HCPs), which have better qualities than conducting polymers (CPs), create a new avenue for the development of intelligent materials with cutting-edge mechanical, optical, and electrical capabilities characteristics, with broader coatings applications [1,2], sensors , catalysis and optics [3-5]. The promising control on physical and chemical properties of metal-conducting polymer nanocomposites by the introduction of nano/metal particles

***Corresponding author email:** Fatima.malk@uobasrah.edu.iq.

ISSN: 1817-2695 (Print); 2411-524X (Online)
Online at: https://jou.jobrs.edu.iq

in conducting polymer matrices are the main interest of scientists [6]. The metal/carbon conducting. Three methods can be used to create polymer nanocomposites. Techniques. :-Initially One includes the dispersion of the metal Particles of nanoparticles into A polymer matrix. Within This instance, decrease of the metal Ions and The procedure of the Polymerization happen sequentially, which causes aggregation of the Particles of nanoparticles that makes This artificial process Frequently challenging and inconvenient. Within The Second approach, Particles of nanoparticles are produced within in situ While The Polymerization that Steer clear of The aggregation, Making them more beneficial. Here The Polymerization response and The synthesis of the Particles of nanoparticles Continue concurrently. The Third technique consists of the Polymerization of the The matrix all around A metal nanocore via utilizing Chemically compatible ligands either polymeric structures , The size, shape, dimensional ratio, dispersion, and alignment of the filler (organic-inorganic) inside the matrix are the main factors influencing the characteristics of hybrid conductive polymers [7-9]. Consequently, the electrical, mechanical, thermal, and optical properties of the conductive polymer matrix are improved by the addition of a second component (the filler). For these reasons, it was used in sensors, Using Polypyrrole with silver granules as hybrid materials in the manufacture of optical sensors By combining a colloidal solution of silver nanoparticles with a pyrrole solution and then polymerizing the monomer block, silver/Polypyrrole hybrid nanoparticles were produced[10]. The in situ polymerization method was also used to create polyaniline nanoparticles (PANi). Different standard approaches were used to characterize these particles. The pyran and quinone ring transitions were validated by absorption measurements. According to the calculated optical band gap of 2.47 eV, this material exhibits an indirect allowed transition [11].
In this study, pure polymers and hybrid polymers with ZnO,Fe_3O_4 and Ag nanomaterials were prepared using core shell polymerization and study of optical and electrical properties

2. Materials and Methods.

Aniline (C_6H_7N) ,Pyrrole(C_4H_5N), methanol, ethanol, citric acid (CA), and ammonium persulfate ($NH_4S_2O_8$) , and $FeCl_3$, were supplied by Shanghai, China-based Sinopharm Chemical Reagent Limited Corporation. None of the chemical reagents required additional purification before use because they were all analytical reagents (AR).

2.1. Preparation of Polyaniline Nanotubes.

Interfacial polymerization was used to prepare polyaniline nanotubes. The organic phase consisted 3.2 ml of aniline dissolved in 10 ml of CCl_4, and the aqueous phase contained 0.8 M of ammonium per sulfate (APS) diluted in 10 ml of 0.1M HCl. After carefully adding the aqueous solution to the organic solution to form two phases, the reaction was allowed to proceed overnight at room temperature. The polymer that was formed in the interface solution was then collected, Wash with DI water, ethanol, and acetone, then dry for three hours at 80 ℃[12].

2.2. Preparation of Poly pyrrole Nanotubes.

0.489 g of $FeCl_3$ was dissolved in a 5 ml solution of methyl orange (MO) and 60 ml DI water with stirring for 30 Min at room temperature . Then 210 µl pyrrole was gradually added to the solution over 10 minutes, and the mixture was kept at -5°C in a static condition for 24 hours. After filtration and washing with DI water and ethanol , the black precipitate was vacuum-dried for 24 hours at 50°C [13].

2.3. Core Shell polymerization

A solution A consisted of 0,18 g of aniline and 25% w/w of nanoparticle (Ag, Fe_3O_4 and ZnO) which were separately sonicated with 10 ml DI for 30 min.. A solution B consisting of (0.45 g of APS dissolved in 10 ml of HCl) was freshly prepared and then drop wise added to the solution A and the mixture was left for 24 hours at room temperature. The PANI@(ZnO,Fe_3O_4,Ag)
were separated using centrifuge, washed with ethanol and acetone and then dried at 50°C 3 hrs.

PPY@(ZnO, Fe_3O_4,Ag) was prepared the same procedure as that used for prepare ppy nanotube. In the first step 25% w/w of nanoparticles (Ag, Fe_3O_4 and ZnO) were separately ultrasonically dispersed with 60 mL of methyl orange.

3. RESULT AND DISCUSSIONS .

3.1. FT-IR

The IR spectrum of polyaniline (PANI) in figure 1showed that the: relatively small peak at 3243 cm^{-1} can be attributed to the (N–H stretching vibration), which represents the electronic extended conjugation of the PANI salt. The peaks at 3116 and 3034 cm^{-1} are attributed to (=C–H stretching vibrations of the aromatic ring). An absorption peak near 1700 cm^{-1} was also noted, which can be attributed to trace amounts of oxalic acid used during the preparation "[13]The peaks at 1548 and 1461 cm^{-1} correspond to the (C=N and C=C stretching vibration modes) of the quinonoid and benzenoid units of PANI (N=Q=N and N=B=N rings), respectively. The peaks in the range of 1284–1228 cm^{-1} can be attributed to the (C–N stretching vibration). The band at 1391 cm^{-1} is assigned to the ($C–N^+$ stretching of the bipolaron structure). In addition, the intensity ratio of the peaks at 1548 and 1461 cm^{-1} represents the quinoid-to-benzenoid structure ratio. The FTIR spectra of core-shell polymerizations of polyaniline with (Ag, ZnO, and Fe_3O_4) nanoparticles in figure 1(a)shows shifts in the main peaks as listed in table 1, confirming the interaction between metal nanoparticles and the reactive sites of polyaniline.

The IR Spectrum of Polypyrrol (PPY) in figure 1(b) shows that the small peak (300-3500 cm^{-1}**)** N–H stretching , Clear characteristic peaks of PPy can The absorption bands at 1547 cm^{-1} and 1460 cm^{-1} corresponded to the C=C and C–C stretching vibration of the PY rings, The bands seen at 1310 cm^{-1} and 1162 cm^{-1} can be attributed sequentially to the C=N bending and C–N stretching vibration. The band at about 1032 cm^{-1} is ascribed to the C–H bending vibration deformation. The C=N–C stretching vibration was evidentially seen at 955 cm^{-1}. The bands observed at 1010 cm^{-1} and 676 cm^{-1} might belong to the out-of-plane ring deformation and N–H vibrations in the polymer[15]. The peak at 550 and 515$cm^{-1}$is the absorption peak of the Fe-O group. Those peak show a decrease in the sharpness of the absorption peak, which indicates that PPy has been successfully composited with Fe_3O_4 nanoparticles. The peak at 1037.2cm^{-1} shows the C-O-C absorption function of stretching vibrations shifting when PPy is added due to changes in energy and the interaction between PPy and Fe_3O_4 Vibration [16], FTIR analysis showed that the pyrrole polymer retained its chemical structure after incorporating the nanoparticles (Ag, ZnO, Fe_3O_4), exhibiting shifts and changes in peak intensity, indicating strong surface interactions between the polymer chain and the nanoparticles, enhancing the physical and electrical properties of the prepared composites .

Table 2 presents the main FTIR peaks for pure Polypyrrol and their hybrid with Ag, ZnO , and Fe_3O_4 nanoparticles.

Table 1. FTIR main peaks of the polyaniline PANI@ Ag, PANI@ZnO and PANI@ Fe3O4 nanoparticles

Functional groups Vibration	**Frequency (cm^{-1})**			
	Polyaniline	**PANI @Ag**	**PANI @ZnO**	**PANI@Fe_3O_4**
N-H	3243	3226	3220	3219
=C-H (aromatic)	3034	3052	3060	3049
C=N (N=Q=N ring)	1548	1565	1563	1558
C=C (N=B=N ring)	1461	1484	1475	1472
C-N	1284	1296	1286	1290

Table 2. FTIR main peaks of the Polypyrrole and Ag, ZnO and Fe3O4 nanoparticles in PANI.

Functional groups Vibration	Frequency (cm^{-1})			
	Polypyrrol	**PPY @Ag**	**PPY @ZnO**	**PPY@Fe_3O_4**
C=C	1541	1540	1533	1527
C-=N	1406	1430	1453	1460
C-C	1310	1300	1288	1290

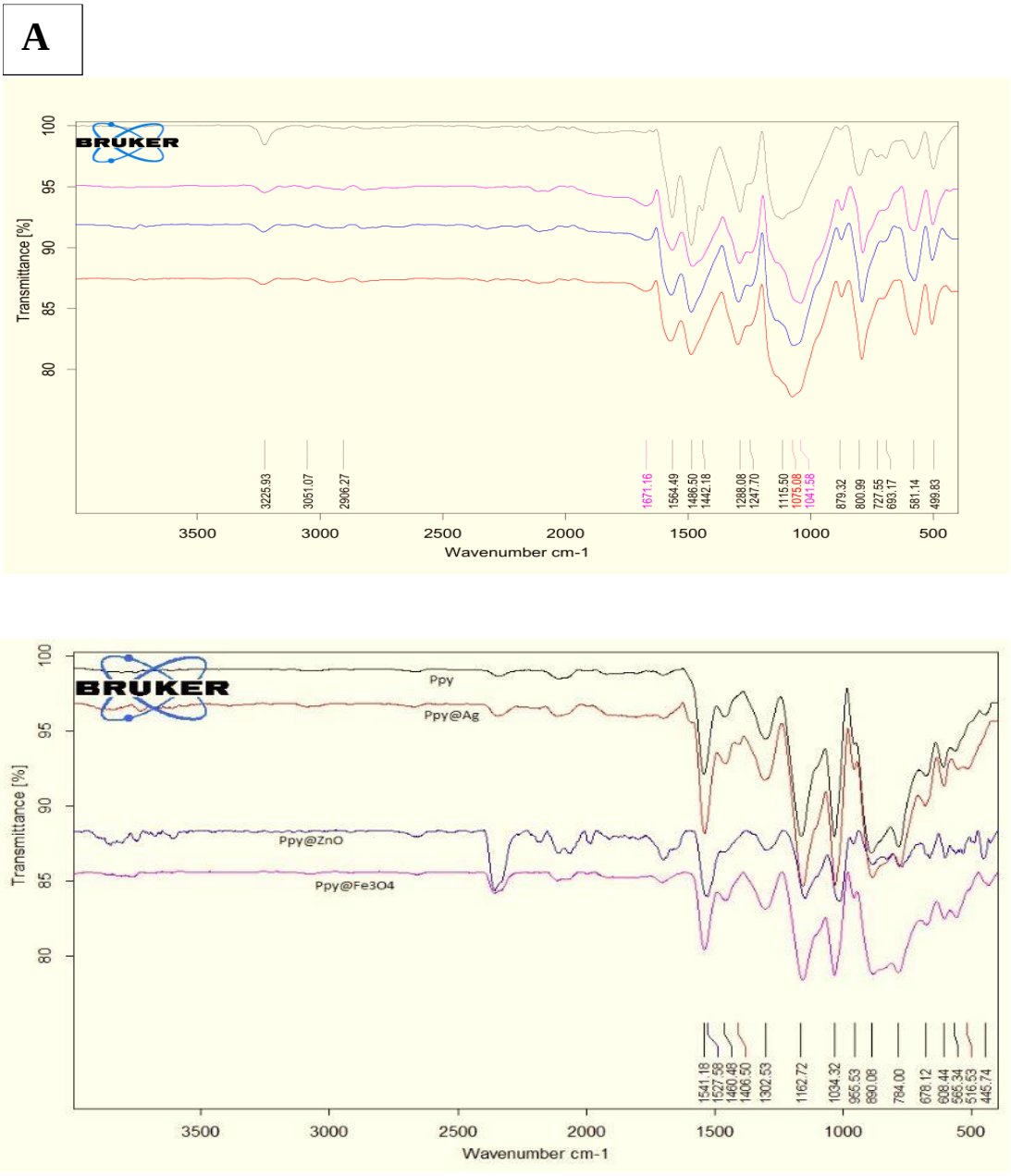

Fig 1. (A) .FT-IR Spectra of PANI @Nanoparticals. (B). FT-IR Spectra of PPY @Nanoparticals

3.2. Morphology.

3.2.1 . Scanning Electron Microscope (SEM)

The scanning electron microscope (SEM) image shows that the prepared material has an interlocking rod-like structure with an irregular distribution, with dimensions within the nanoscale figure 2. (a).figure 2.(B), High-magnification scanning electron microscopy (SEM) images show that the particles are spherical, with nanoscale sizes ranging from (80 to 150 nm), and exhibit agglomeration due to high surface energy. The surface roughness indicates either a polymer coating over the particles or a Core @Shell structure, fig 2. (C): shows quasi-spherical nanoparticles clustered in cauliflower-like morphology. This type of structure indicates multinuclear growth with small primary particles clumping together to form larger aggregates fig 2. (D) shows larger, more compact particles, with clear boundaries between grains, indicating partial fusion between particle . Fig 3. (A),shows a rod-like structure representing the core, consisting of an interconnected network of Polypyrrol fibres with a relatively rough surface. This structure forms the basic support of the composite. In Fig3.(B): appearance of quasi-spherical nanoparticles distributed on the surface of the polymer fibres is observed, indicating the formation of a shell around the polymer core. This relatively uniform surface distribution indicates the success of the coating or deposition process, where the PPY fibres act as a template for the growth of ZnO particles. Thus, a PPY core structure is formed, surrounded by a ZnO shell. In Fig 3 (C) PPY @ Ag, small particles with high electron density are observed attached to the surface, indicating the formation of a partial metallic shell or nanoparticles encapsulating the fibres. In Fig 3(D) integration between the components is shown, resulting in a denser and more compact structure, indicating the formation of a multi-layer core-shell system. The SEM pictures generally show that a Core @shell type nanostructure was successfully formed, with a good distribution of nanoparticles surrounding the polymer matrix, allowing for usage in electrochemical or sensory applications [17,18].

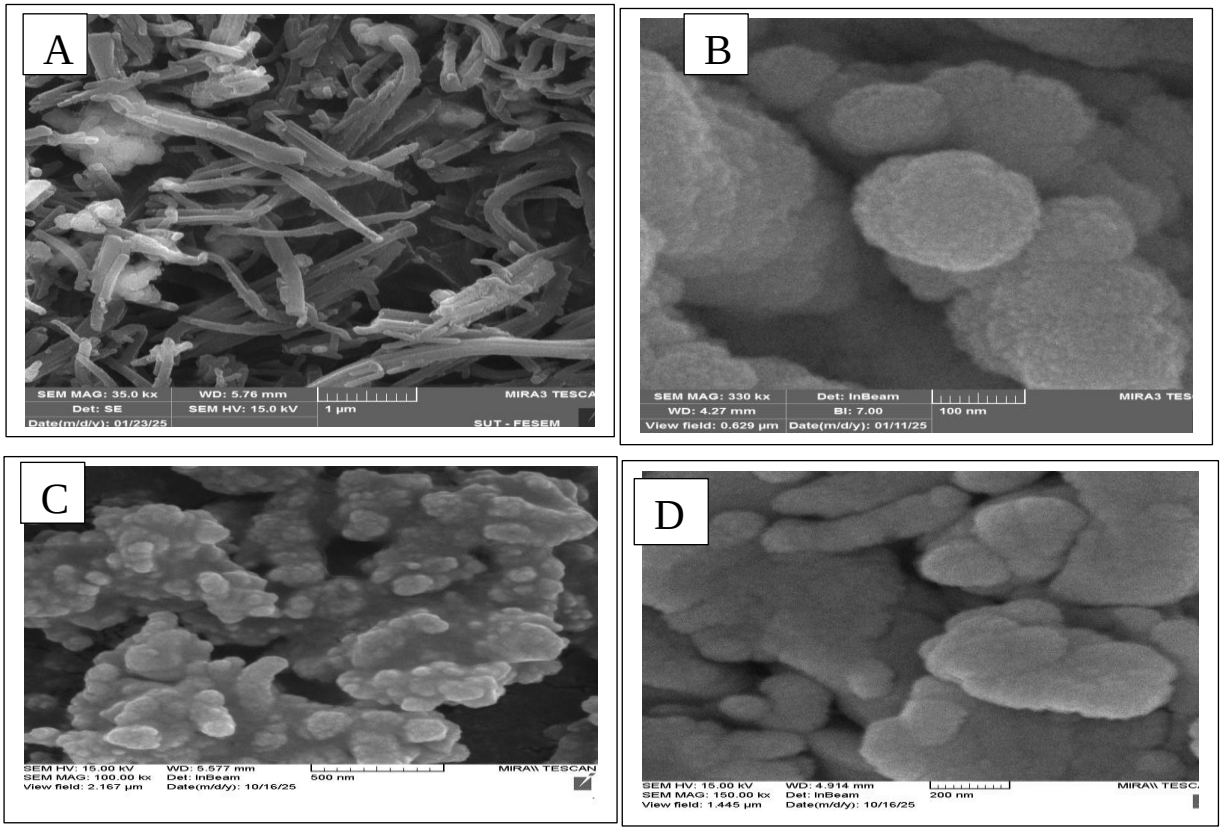

Fig .2 . Scanning Electron Microscope (SEM) of
A- PANI . B-PANI@ZnO C- PANI@Ag D-PANI@Fe_3O_4

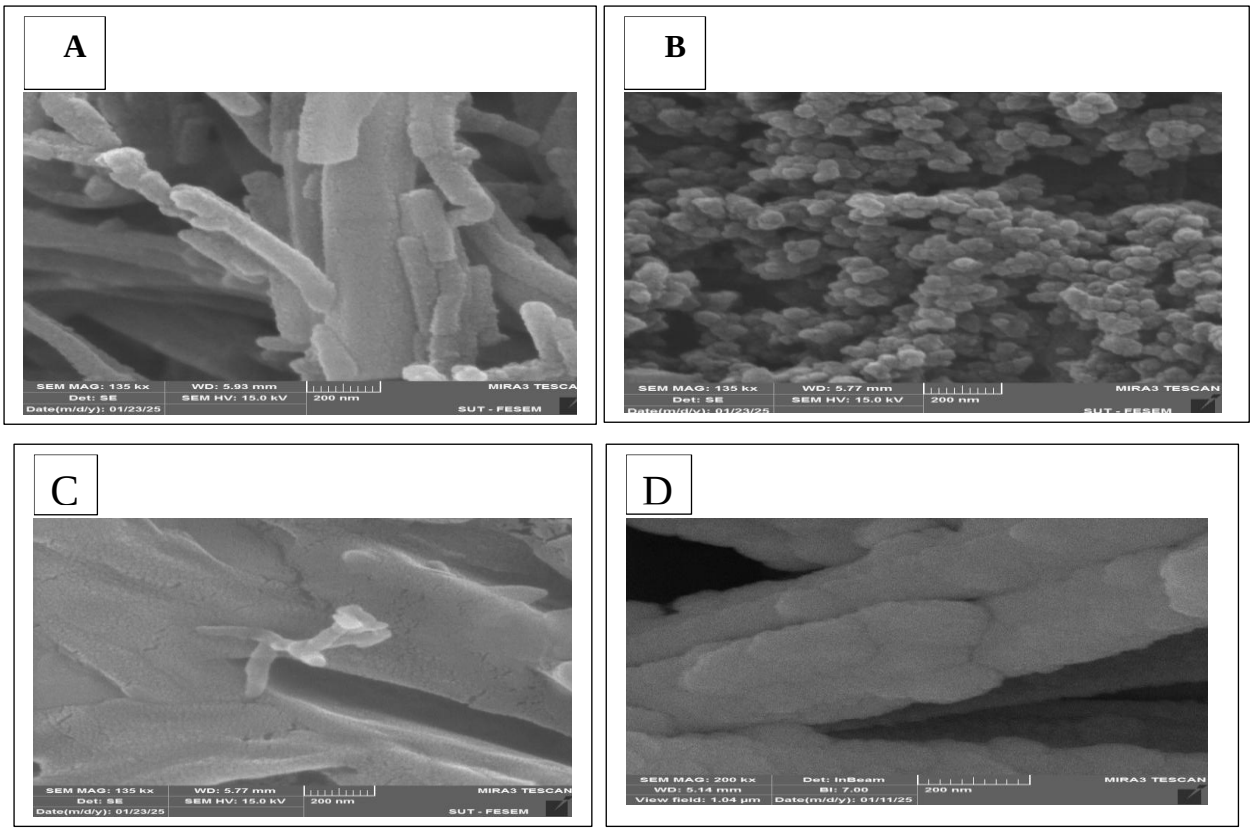

Fig. 3. Scanning Electron Microscope (SEM) of A-PPY, B- PPY@ZnO , C-PPY@Ag D-PPY@Fe_3O_4.

3.2.2. Transmission Electron Microscope (TEM).

Transmission electron microscopy (TEM) analysis Shows the morphological changes of polyaniline (PANI) and Poly pyrrole (PPY) . Figure (4) before and after core shell formation . Fig (4A) exhibits a nanotube structure of polyaniline, where the tubules appear relatively homogeneous and interconnected, indicating successful synthesis and the formation of a high-surface-area nanostructure—a property crucial for enhancing electrical conductivity and increasing surface interaction sites. In Figure (4 B), a clear variation in electron density is observed as a result of the introduction of zinc oxide (ZnO) into the polymer matrix, where dark areas appear indicating inorganic particles distributed within PANI, Figure (4 D): also shows the distribution of (Fe_3O_4) particles within the polymer structure, where the particles appear more homogeneous compared to the pure sample, indicating effective integration between the organic and inorganic phases.

In figure (5) :introduction of inorganic nanoparticles into PPY leads to a marked change in morphology, an increase in electron density, and an improvement in structural regularity. These structural changes are typically reflected in improved electrical, electrochemical, or sensory properties compared to the pure polymer, thus confirming the success of the preparation and formation of nanocomposites.

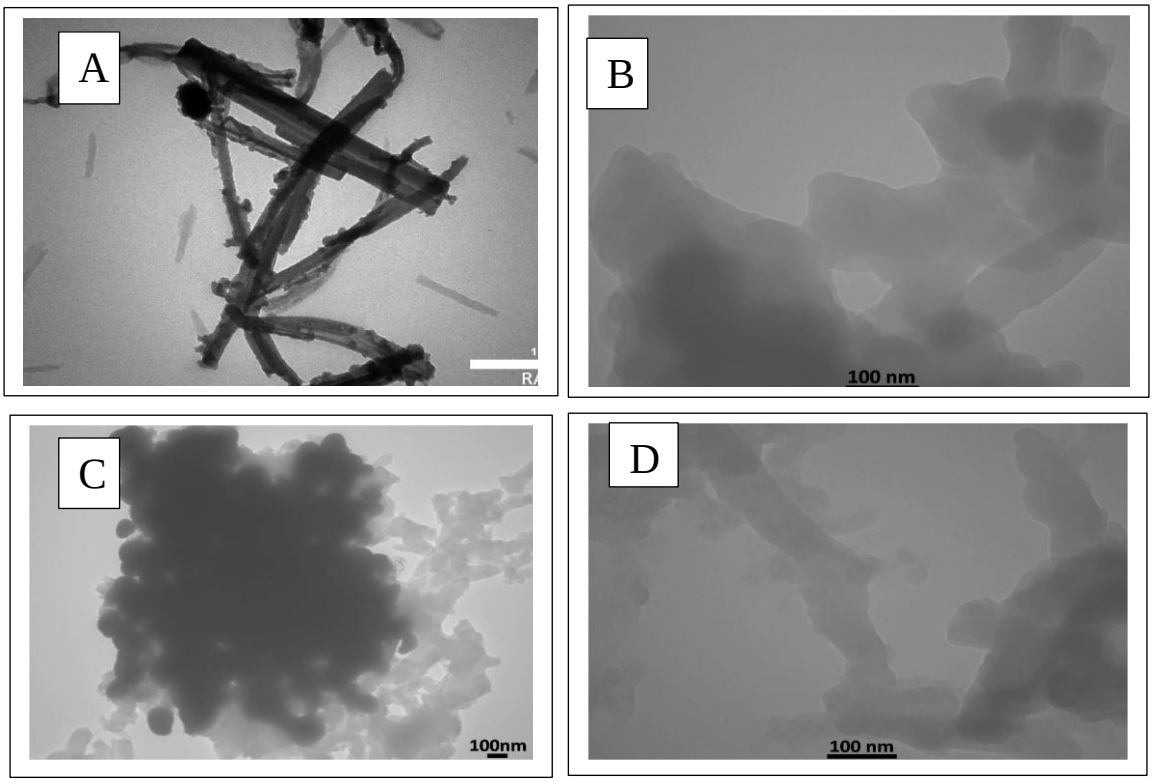

Fig. 4 . Transmission Electric Microscopy (TEM) of A-PANI pure ,B- PANI @ZnO, C- PANI @Ag, D- PANI@Fe_3O_4

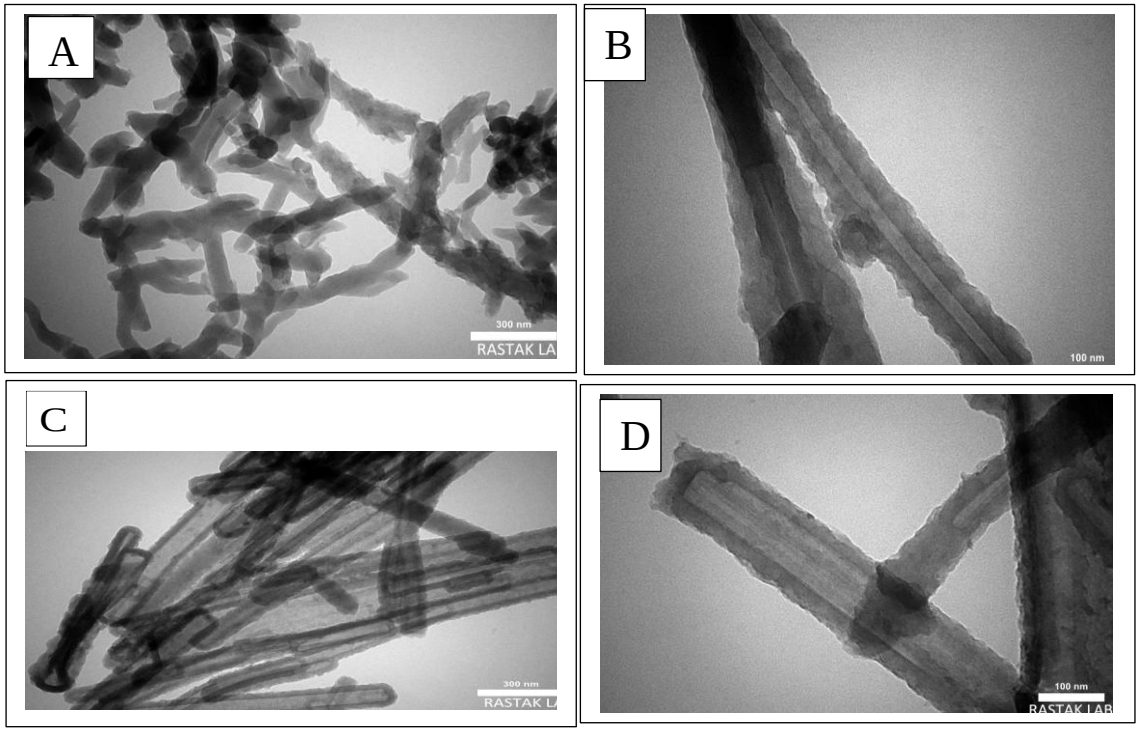

Fig. 5 . Transmission Electric Microscopy (TEM) of A-PPY pure , B- PPY @ZnO, C- PPY @Ag, D- PPY@Fe_3O_4.

3.3. UV–Visible Spectra of Polyaniline, Polypyrrole and Its Core–Shell Polymers

The UV-Visible spectra of polyaniline, Polypyrrole and their core@ shell polymerization with Ag,Fe_3O_4 and ZnO nanoparticles are showed in figure (6) and (7) respectively. two main electronic transition (n→ π*) and (π → π*) are observed In Figure 6 , the peaks at (250–300) nm are attributed to (π → π*) ,while the peaks at (350-450) nm are attributed to (n→ π*) transition of the benzenoid rings in the polyaniline chain, representing the electronic transition from the HOMO to LUMO in the benzenoid units.High absorption intensity was observed for PANI @ZnO and PANI @Fe_3O_4 rather than PANI @Ag and the all hybrid polymers had high absorption than pure polyaniline attributed to effect of nanoparticles interaction with polyaniline for core @ shell polymers [19,20].
In Figure 7: For pure PPy characteristic absorption peaks are observed at 250 nm and 384 nm. These peaks correspond to the electronic transitions from the highest occupied molecular orbital (HOMO) to the lowest unoccupied molecular orbital (LUMO), specifically attributed to π–π* transitions in the conjugated polymer backbone . transition a wide band was observed as a result of boron transport due to oxidative polymerization in those at (350–500) nm. PANI@ZnO particles exhibited high absorption and a broad peak compared to PANI @ Ag, PANI@Fe_3O_4, and pure polyaniline. This is attributed to the interaction of the nanoparticles with Polypyrrol in core-shell polymers, Because the particles are magnetic, the absorbance of PPY@Fe_3O_4 is lower than that of pure Polypyrrol [21,22].

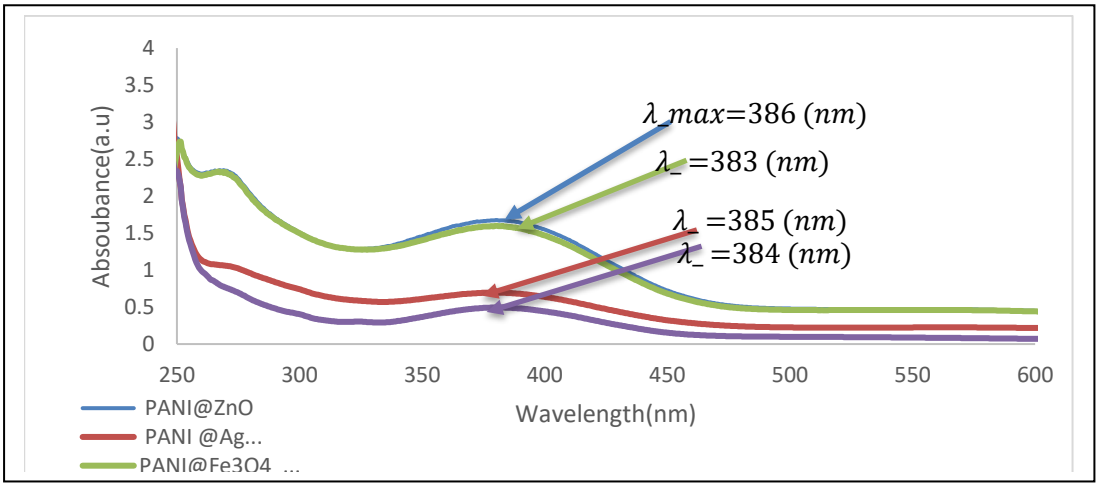

Fig 6. UV-Visible spectra of Polyaniline pure and polyaniline@ nanoparticles

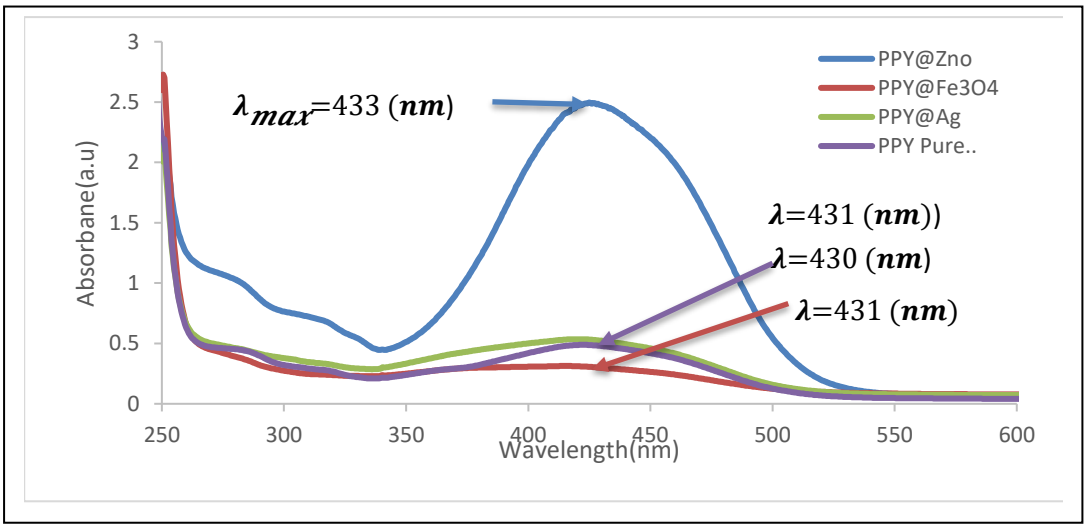

Fig. 7. UV-Visible spectra of PPY pure and PPY@ nanoparticles

3.3.1. Optical Absorption coefficient and Optical Energy Gap.

To determine the type of electronic transfer that takes place in the substance's electronic structure, the absorption coefficient is especially important in the absorption area . The following equation was used to determine the absorption coefficient [23].

$$\alpha = \frac{1}{d}\ln\left[\frac{(1-R)^2}{2T} + \sqrt{\frac{(1-R)^4}{4T^2} + R^2}\right] \ldots \quad (1)$$

Reflection and transmittance are represented by the indices R and T, respectively. and d is the expression for the film thickness, R was computed using the following formula:-

$$R = 1 - \left(\sqrt{\frac{T^*}{EXP(-a)}}\right) \ldots \quad (2)$$

The mass of the glass substrate (m_1) and the polymers layer on that substrate (m_2), as explained below, are included in the standard method used to get the latter parameter.

$$d = \frac{m_2 - m_1}{\rho a} \ldots \quad (3)$$

The symbols (ρ) and (a) stand for the dye density and sample area, respectively.
Since the absorption coefficient (α) values exceed 10^4 cm^{-1}, the electronic transitions are of the direct kind. Consequently, The absorption coefficient becomes very important in the absorption band. Identify the kind of electronic transmission that takes place in the electronic [24],Figure (8,9) , Absorption coefficient of Polyaniline pure and polyaniline@ nanoparticles and Absorption coefficient of PPY pure and PPY@ nanoparticles.
Induction of a separate, hole, uncorrelated free electron with the least amount of energy is known as the optical gap. The mobility of individual particles in solids is linked to the energy gap effect. The energy gap estimates in this study are computed using the x-axis's intercept of (against h). Tauc's relationship, which is defined in Eq. 4 below, is applied to characterize the latter treatment, Figure (10-13) [24] .

$$\alpha h\nu = A(h\nu - E_g)^r \ldots \quad (4)$$

where r is the distribution of the density of states index, which varies depending on the transition mode (direct or indirect), and represents the transition probability dependent constant[24].

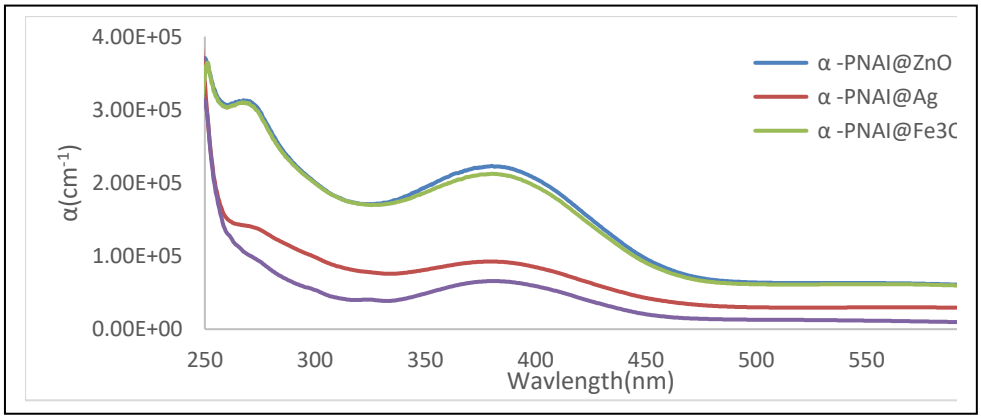

Fig. 8. Absorption coefficient of Polyaniline pure and polyaniline@ nanoparticle

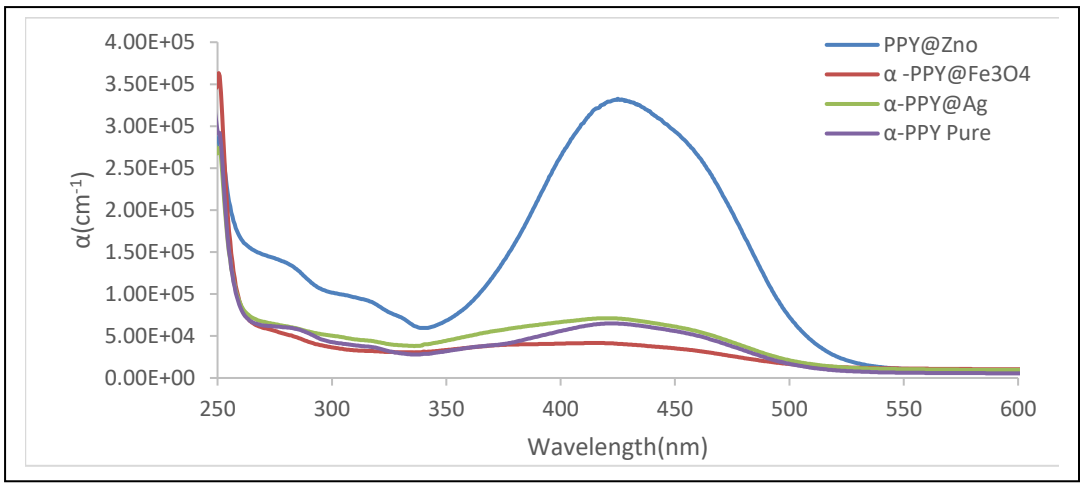

Fig. 9. Absorption coefficient of PPY pure and PPY@ nanoparticles

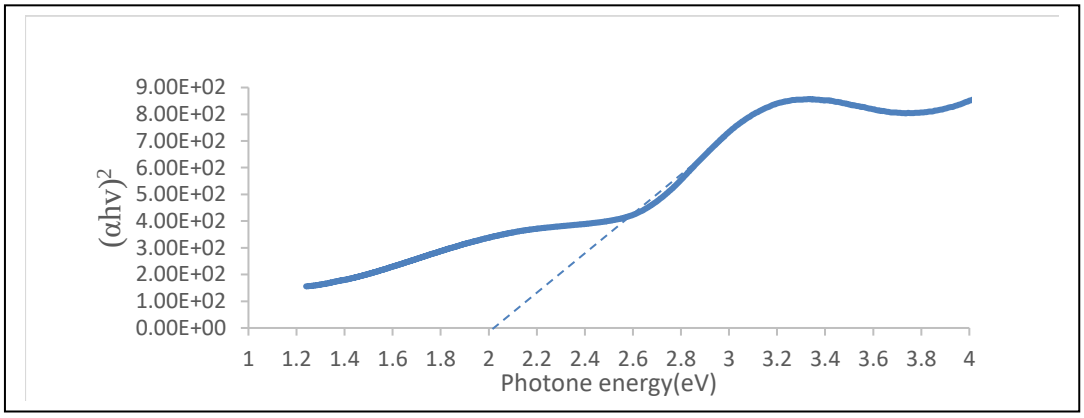

Fig.10. Optical energy gap of PANI @ZnO

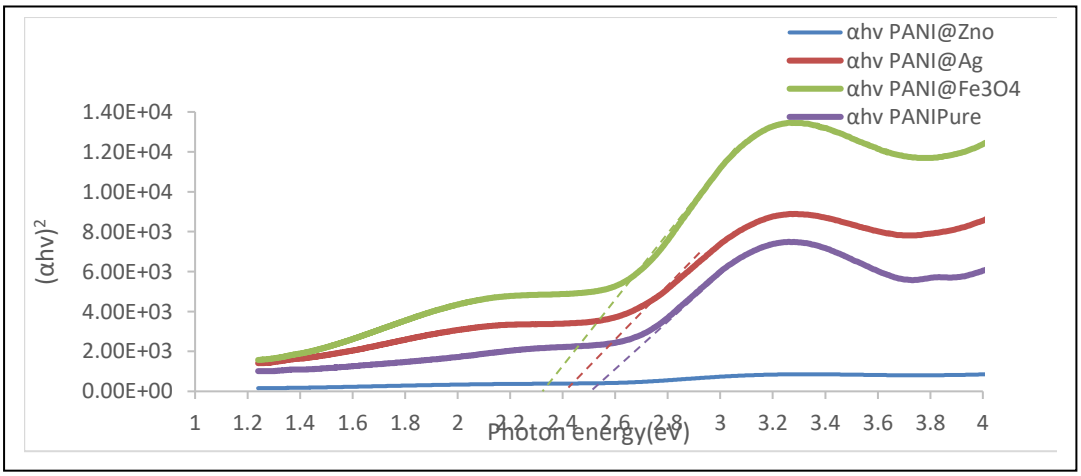

Fig. 11. Optical energy gap of PANI@ nanoparticles

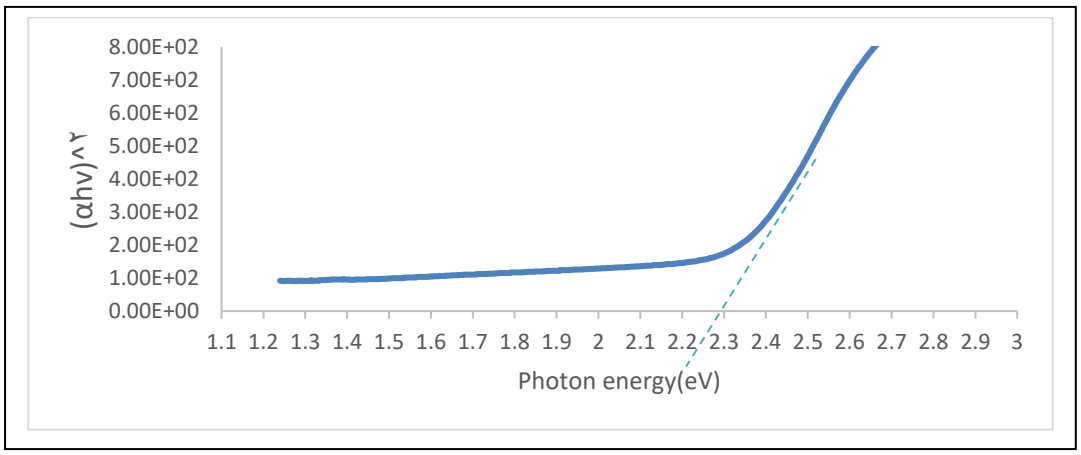

Fig. 12. Optical energy gap of PPY@ZnO

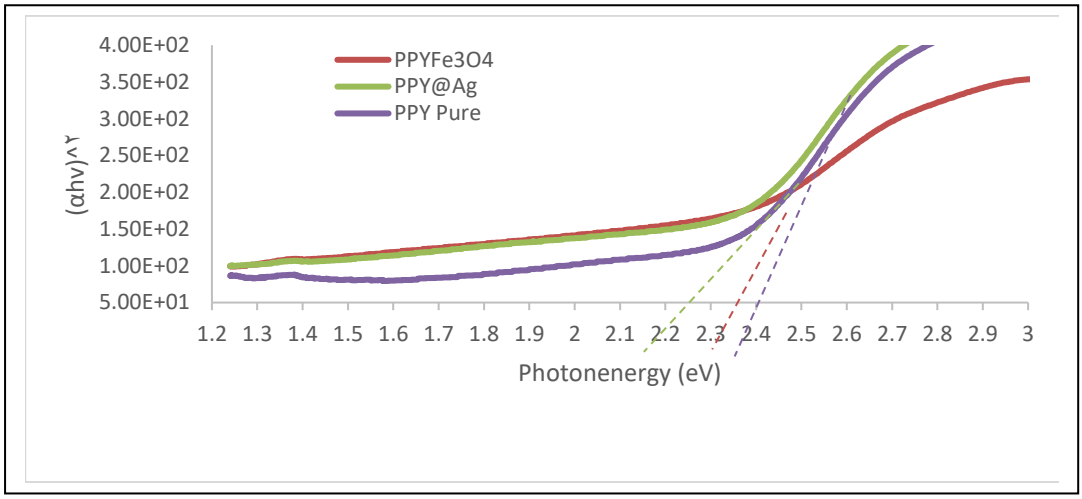

Fig. 13. Optical energy gap of PPY@ nanoparticles

3.4. Characteristic (I-V)

The I-V characteristic of polyaniline and its core@ shell polymers in figure 14. and, poly pyrrole and its core@ shell polymers in figure 15. were studied to determine how electricity travels in polymer membranes and showed that the a quasi-linear relationship between current and voltage, which indicates ohmic behavior, meaning that the electrical conductivity is stable and there are no large barriers that impede the transfer .

Figure 14. shows the lowest current value at all applied voltages, indicating that electrical conductivity is relatively limited due to the lack of charge carriers and the presence of a larger energy gap of polyaniline compared to Core@ Shell polymers [25],Due to the inclusion of highly conductive silver particles, which aid in the creation of new electron transport channels and improve charge mobility inside the polymer, PANI @Ag displays a greater current than pure PANI. Compared to both pure PANI and PANI @Ag, PAN I@ Fe_3O_4 exhibits a greater current. This is explained by the interaction between PANI and Fe_3O_4 particles, which leads to increased charge carrier density and enhanced conductivity through hopping, The best electrical conductivity of all the samples is demonstrated by PANI @ZnO, which shows the highest current values at all voltages. This is because of: PANI and ZnO have a strong interaction Improved charge transfer at the interface Low resistance to the substance overall ,Possible decrease in the band gap[26].

Figure 15. Shows the least amount of current across all voltages. This shows that pure PPY has little electrical conductivity due to its high internal resistance and absence of charge carriers. When compared to pure PPY, the current is marginally better. This is explained by ZnO function as a semiconductor, which enhances charge transfer; nevertheless, compared to metallic materials, ZnO semiconducting nature limits the effect [27] .PPY@Fe_3O_4 At all voltage, it captures highest current values. as conductive polymers are supplemented with nanoparticles, their electrical conductivity significantly improves as compared to the pure polymer, according to current-voltage (I-V) measurements. For every sample, the curves show ohmic behavior. Using the following formula, the electrical conductivity was also determined : [27]

$$\sigma = \frac{d}{R*A} \ldots \quad (4)$$

When: σ: Electrical conductivity (S/cm or S/m), A: Cross-sectional area of the material (cm^2 or m^2), R: Electrical resistance (Ω), d: Film thickness(mor cm).

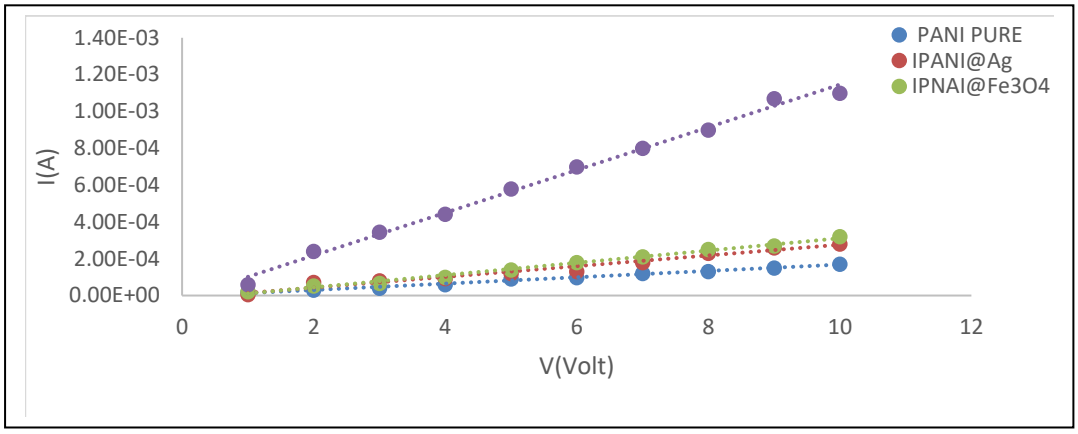

Fig. 14. I-V curve of the PANI and PANI @Nanoparticls

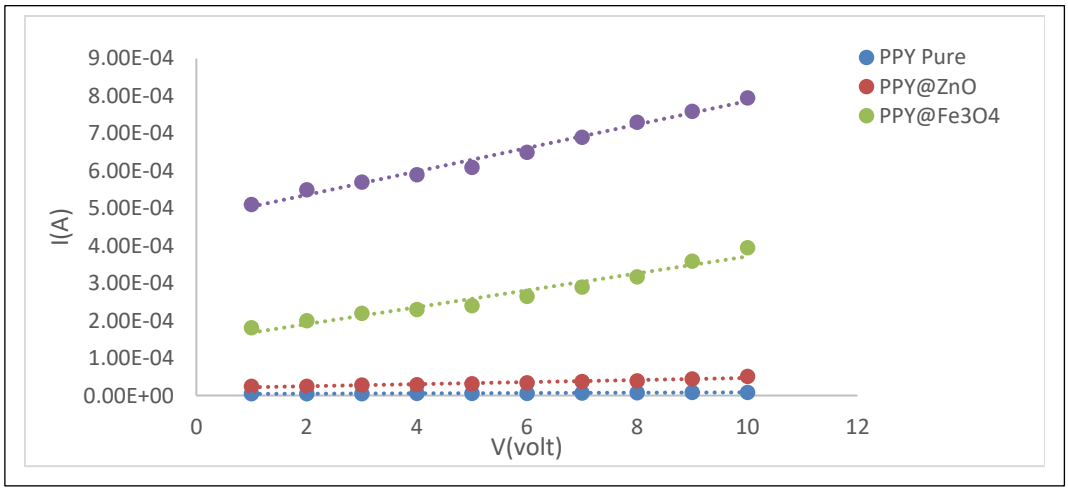

Fig. 15. I-V curve of the PPY and PPY @ nanoparticles

Table 3. represents the electrical conductivity and optical energy gap for all polymers.

Polymers	E g (eV)	σ (S/m)
PANI	2.5	$156x10^{-4}$
PANI @ZnO	2.2	$780x10^{-4}$
PANI @Ag	2.4	$288x10^{-4}$
PANI@Fe_3O_4	2.31	$273x10^{-4}$
PPY	2.37	$429x10^{-6}$
PPY @Zno	2.21	$331x10^{-5}$
PPY @Ag	2.15	$273x10^{-4}$
PPY@Fe_3O_4	2.3	$253x10^{-4}$

4. Conclusion

The hybrid polymers prepared using core shell polymerization showed that the rise in absorption strength and a Red shift, indicating a decrease in the energy gap, which was connected to the improvement in electrical characteristics and UV-Vis optical properties. The observed increase in electric current is directly correlated with a smaller energy gap, which promotes electron excitation and migration, The technique of electrical transport is also significantly influenced by the type of nanoparticles, These materials are promising for electro electronic applications, such as sensors, electrodes, and photodetectors, as reinforcing conductive polymers with nanoparticles modifies their electronic structure and improves charge transfer. This is generally confirmed by the clear agreement between the optical properties results and the electrical conductivity measurements.

References

[1] K. Madali and M. Adrine, "In situ synthesis of polypyrrole/Nd-doped ZnO nanocomposite with enhanced visible light photocatalytic performance for the degradation of organic dyes," *Materials Chemistry and Physics*, vol. 296, p. 127248, Feb. 2023, DOI: 10.1016/j.matchemphys.2022.127248.

[2] U. F. Natasha, A. D. Muchammad, I. Irkham, P. Allyn, R. E. Diana, and Y. M. Jacob, "Doping of rare earth element: The effects in elevated physical and optical properties of ZnO," *Talanta Open*, vol. 11, p. 100411, Aug. 2025, DOI: 10.1016/j.talo.2025.100411.

[3] Y. Xu, J. Ma, H. Yu, H. Xu, Y. Wang, D. Qi, and W. Wei, "A simple and universal strategy to deposit Ag/polypyrrole on various substrates for enhanced interfacial solar evaporation and antibacterial activity," *Chemical Engineering Journal*, vol. 384, p. 123379, Mar. 2020, DOI: 10.1016/j.cej.2019.123379.

[4] T. Gabriela, P. D. Lucian, M. L. Eduard, I. Ion, and V. M., "A comparative study of polypyrrole and Ag/polypyrrole hybrid nanocomposites as sensitive material used for new dry polarizable bioimpedance sensors," *Applied Sciences*, vol. 11, p. 4168, 2021, DOI: 10.3390/app11094168.

[5] K. T. Fraczek, M. Z. Krzywaznia, A. J. Ociepka, Z. Rucki, and Z. Szczepanik, "Measurements of electrical impedance of biomedical objects," *Acta of Bioengineering and Biomechanics*, vol. 18, pp. 11–17, 2016, DOI: 10.5277/ABB-00294-2015-03.

[6] M. Moniruzzaman, S. Sahoo, D. Ghosh, C. K. Das, and R. Singh, "Preparation and characterization of polypyrrole/modified multiwalled carbon nanotube nanocomposites polymerized in situ in the presence of barium titanate," *Journal of Applied Polymer Science*, vol. 128, pp. 698–705, Apr. 2013, DOI: 10.1002/app.38202.

[7] L. Sajid and A. Sharif, "Recent development in hybrid conducting polymers: Synthesis, applications and future prospects," *Journal of Industrial and Engineering Chemistry*, vol. 60, pp. 53–84, 2018, DOI: 10.1016/j.jiec.2017.09.038.

[8] Y. Yuwei, Z. Haichao, W. Chunting, Z. Dawei, C. Hao, and L. Wei, "Design of novel superhydrophobic aniline trimer modified siliceous material and its application for steel protection," *Applied Surface Science*, vol. 457, pp. 752–763, Nov. 2018, DOI: 10.1016/j.apsusc.2018.06.135.

[9] Z. Sukun, W. Meng, C. Xiong, and X. Feng, "Facile template synthesis of microfibrillated cellulose/polypyrrole/silver nanoparticles hybrid aerogels with electrical conductive and pressure responsive properties," *ACS Sustainable Chemistry & Engineering*, vol. 3, pp. 1–5, Nov. 2015, DOI: 10.1021/acssuschemeng.5b01020.

[10] Y. Wang, S. M. Zhang, and Y. Deng, "Flexible low-grade energy utilization devices based on high-performance thermoelectric polyaniline/tellurium nanorod hybrid films," *Journal of Materials Chemistry A*, vol. 9, pp. 3157–3568, Mar. 2016, DOI: 10.1039/C6TA01140C.

[11] M. Hongyu, Z. H. Xiaogang, Y. Xiangguo, and Y. Sudong, "Preparation and enhanced capacitance of core-shell polypyrrole/polyaniline composite electrode for supercapacitors," *Journal of Power Sources*, vol. 176, pp. 403–409, Jan. 2008, DOI: 10.1016/j.jpowsour.2007.10.070.

[12] B. Ch. Ram and N. Debashish, "Tailoring the properties of 2-D rGO-PPy-ZnS nanocomposite as emissive layer for OLEDs," *Optik*, vol. 231, p. 166336, Apr. 2021, DOI: 10.1016/j.ijleo.2021.166336.

[13] R. P. Singh, A. Tiwari, and A. C. Pandey, "Silver/polyaniline nanocomposite for the electrocatalytic hydrazine oxidation," *Journal of Inorganic and Organometallic Polymers and Materials*, vol. 21, pp. 788–792, Aug. 2011, DOI: 10.1007/s10904-011-9554-y.

[14] L. María, C. Amanda, J. Ana, O. Amelia, M. Jorge, C. E. Guerrero, and N. Natalia, "Synthesis and novel purification process of PANI and PANI/Ag NPs composite," *Molecules*, vol. 24, p. 1621, Apr. 2019, DOI: 10.3390/molecules24081621.

[15] J. Mahmood, N. Arsalani, S. N. Hamed, Z. Hanif, and K. E. Geckeler, "Preparation and characterization of hybrid polypyrrole nanoparticles as a conducting polymer with controllable size," *Scientific Reports*, vol. 14, p. 11653, May 2024, DOI: 10.1038/s41598-024-61587-1.

[16] P. Simamora, M. Manullang, J. Munthe, and J. Rajagukguk, "The structural and morphology properties of Fe3O4/PPy nanocomposite," *Journal of Physics: Conference Series*, vol. 1120, no. 1, p. 012063, Nov. 2018, DOI: 10.1088/1742-6596/1120/1/012063.

[17] N. Turkten, Y. Karatas, and M. Bekbolet, "Preparation of PANI modified ZnO composites via different methods: Structural, morphological and photocatalytic properties," *Water*, vol. 13, p. 1025, Apr. 2021, DOI: 10.3390/w13081025.

[18] V. Arunima, K. Tanuj, and S. Rahul, "Silver doped polypyrrole nanocomposite-based gas sensor for enhanced ammonia gas sensing performance at room temperature," *Chemical Physics Impact*, vol. 9, p. 100722, Dec. 2024, DOI: 10.1016/j.chphi.2024.100722.

[19] T. Jabeen, M. Rashid, A. Khan, *et al*., "A comparative analysis of the removal of arsenic from water using magnetite/polyaniline-polypyrrole nanocomposite," *International Journal of Environmental Science and Technology*, vol. 22, pp. 14519–14538, May 2025, DOI: 10.1007/s13762-025-06573-4.

[20] P. Shilpa, Y. T. Gutte, and C. H. Birajdar, "Investigating the physicochemical and optical properties of PANI and PANI-ZnO thin films for an efficient ammonia sensor at ambient conditions," *Research Square*, vol. 18, pp. 1–16, Jul. 2024, DOI: 10.21203/rs.3.rs-4603844/v1.

[21] L. Cong, M. Irfan, W. Abbas, F. M. A. Alzahrani, S. Alamri, and M. Imran, "Structural, electrical, and optical characteristics of polypyrrole-doped DBSA/ZrO_2 nanocomposites," *Discover Materials*, vol. 6, p. 89, 2026, DOI: 10.1007/s43939-026-00556-z.

[22] H. M. Jawad, "Theoretical study of the electronic and optical properties of polypyrrole (PPy) polymer nanoparticles doped with TiO_2 and ZnO," *Journal of Nano Materials Impact*, vol. 1, pp. 1–6, Oct. 2025, DOI: 10.71109/nmi.2025.1.1.3.

[23] H. M. Fatima, T. H. Alaridhee, and A. A. Al-Saeed, "Effects of static magnetic field on dye extracted from anchusa-italica through optimization the optoelectronic properties," *International Journal of Nonlinear Analysis and Applications*, vol. 12, pp. 949–960, Dec. 2021, DOI: 10.22075/IJNAA.2021.5158.

[24] H. M. Fatima, J. S. Zainab, and A. B. H. Alyaa, "Absorption, extinction coefficient and energy gap of PVA/starch doping Rhodamine-B," *AIP Conference Proceedings*, vol. 2834, p. 030012, 2023, DOI: 10.1063/5.0161526.

[25] A. K. Kar and S. Dey, "Morphological and optical properties of polypyrrole nanoparticles synthesized by variation of monomer to oxidant ratio," *Materials Today: Proceedings*, vol. 18, pp. 1072–1076, 2019, DOI: 10.1016/j.matpr.2019.06.566.

[26] N. A. NiazAbdul and S. F. Hussain, "Structural and electronic properties of PANI-ZnO-TiO_2 nanocomposite," *Journal of Ovonic Research*, vol. 18, pp. 713–722, Nov. 2022, DOI: 10.15251/JOR.2022.185.713.

[27] M. Khalid, A. M. Tumelero, I. S. Brandt, V. C. Zoldan, J. J. S. Acuña, and A. A. Pasa, "Electrical conductivity studies of polyaniline nanotubes doped with different sulfonic acids," *ISRN Materials Science*, vol. 2013, p. 718304, Nov. 2013, DOI: 10.1155/2013/718304.

Journal of Basrah Researches (Sciences) **52**(1), 254 (2026)
DOI: https://doi.org/10.56714/bjrs.52.1.18

الخواص الكهربائية والبصرية لأنابيب PPy و PANI النانوية المحضرة بواسطة بلمرة اللب والقشرة باستخدام جسيمات نانوية من الفضة وأكسيد الزنك وأكسيد الحديد الثلاثي

فاطمة حميد مالك[1،*]، حسين فالح حسين[2]، صلاح شاكر اللعيبي[3]

[1]مركز أبحاث البوليمرات، جامعة البصرة
[2]قسم الفيزياء، كلية التربية للعلوم الصرفة، جامعة البصرة
[3]قسم الكيمياء، كلية العلوم، جامعة البصرة

معلومات البحث

الاستلام	26 اذار 2026
المراجعة	01 أيار 2026
القبول	07 أيار 2026
النشر	30 حزيران 2026

الكلمات المفتاحية

نواة - قشرة، الخصائص الكهربائية، الخصائص البصرية، PPY، PANI، الموصلية الكهربائية.

Citation: F. H. Malk et al., J. Basrah Res. (Sci.) **52**(1), 254 (2026). DOI:https://doi.org/10.56714/bjrs.52.1.18

الملخص

. تم تحضير أنابيب نانوية من البوليبيرول (PPy) والبولي أنيلين (PANI) بتقنية البلمرة ذات البنية الأساسية المغلفة (core@shell) باستخدام جسيمات نانوية من أكسيد الزنك (ZnO) والفضة (Ag) وأكسيد الحديد الثلاثي (Fe_3O_4) لإنتاج بوليمرات هجينة، وهي PPy@(ZnO, Ag, Fe_3O_4) و PANI@(ZnO, Ag, Fe_3O_4). وتم توصيف هذه البوليمرات الهجينة باستخدام مطيافية الأشعة تحت الحمراء (IR) لتأكيد تركيبها الكيميائي، وباستخدام المجهر الإلكتروني الماسح والنافذ (SEM و TEM) لتأكيد شكلها وبنية الأنابيب النانوية.

كما دُرست الخصائص البصرية لهذه البوليمرات الهجينة باستخدام مطياف الأشعة فوق البنفسجية والمرئية. أظهرت الأطياف قمم امتصاص واسعة في نطاق (383-386) نانومتر و(430-433) نانومتر لـ PANI@ZnO,Fe_3O_4,Ag و PANI@ZnO,Fe_3O_4,Ag على التوالي، ووجد أن فجوات الطاقة لـ PANI النقي تبلغ 2.37 إلكترون فولت و2.5 إلكترون فولت لـ PPY و PANI على التوالي، كما أظهرت انخفاض فجوة الطاقة مع دمج الجسيمات النانوية.

دُرست خصائص التيار-الجهد لـ PANI و PPy وبوليمراتهما ذات البنية الأساسية-الغلافية مع جسيمات ZnO,Fe_3O_4 و Ag النانوية لتحديد كيفية انتقال الكهرباء في أغشية البوليمر. أظهرت النتائج علاقة شبه خطية بين التيار والجهد، مما يشير إلى سلوك أومي، أي أن التوصيل الكهربائي مستقر ولا توجد عوائق كبيرة تعيق انتقاله. لوحظت أعلى موصلية لـ PANI@Zn ($780x10^{-4}$ سيمنز/متر) و PPY@Ag ($273x10^{-4}$ سيمنز/متر).

***Corresponding author email:** Fatima.malk@uobasrah.edu.iq.

ISSN: 1817-2695 (Print); 2411-524X (Online)
Online at: https://jou.jobrs.edu.iq